2005

Fragmentation Dynamics of H2S Following S 2p Photoexcitation

Renaud Guillemin
CNRS, Laboratoire de Chimie Physique-Matière et Rayonnement

S-W Yu
Lawrence Berkeley National Laboratory

Wayne C. Stolte
University of Nevada, Las Vegas, wcstolte@lbl.gov

Dennis W. Lindle
University of Nevada, Las Vegas, lindle@unlv.nevada.edu

Fragmentation dynamics of H2S following S 2p photoexcitation

R. Guillemin, W. C. Stolte, L. T. N. Dang, S.-W. Yu, and D. W. Lindle

Citation: J. Chem. Phys. **122**, 094318 (2005); doi: 10.1063/1.1860012
View online: http://dx.doi.org/10.1063/1.1860012
View Table of Contents: http://jcp.aip.org/resource/1/JCPSA6/v122/i9
Published by the American Institute of Physics.

Fragmentation dynamics of H_2S following S 2*p* photoexcitation

R. Guillemin, W. C. Stolte, and L. T. N. Dang
Department of Chemistry, University of Nevada, Las Vegas, Nevada 89154-4003

S.-W. Yu
Department of Chemistry, University of Nevada, Las Vegas, Nevada 89154-4003
and Center for X-Ray Optics, Lawrence Berkeley National Laboratory, Berkeley, California 94720

D. W. Lindle
Department of Chemistry, University of Nevada, Las Vegas, Nevada 89154-4003

(Received 22 October 2004; accepted 27 December 2004; published online 4 March 2005)

The fragmentation dynamics of core-excited H_2S has been studied by means of partial anion and cation yield measurements around the S $L_{2,3}$-subshell ionization thresholds. All detectable ionic fragments are reported, and significant differences between partial ion yields are observed. Possible dissociation pathways are discussed by comparison to previous studies of electron spectra. © *2005 American Institute of Physics*. [DOI: 10.1063/1.1860012]

I. INTRODUCTION

The rapid development of synchrotron-radiation instrumentation culminating in third-generation facilities has opened new opportunities for high-resolution studies of core-level molecular spectroscopy. The energy selectivity achieved by monochromators allows selective excitation of different types of molecular states with a photon bandwidth narrower than the natural width of the core-excited states. In this context, core excitation of small molecules with repulsive intermediate states draws a lot of attention because nuclear motion can play a significant role within the lifetime of the excited states, typically in the 10^{-14} s range. In some cases, neutral molecular dissociation faster than electronic decay has been evidenced. In pioneering work, Morin and Nenner observed sharp atomic decay lines in the resonant-Auger spectrum of the HBr molecule upon $3d \rightarrow \sigma^*$ excitation due to ultrafast molecular dissociation.[1] In contrast, dissociation slower than electronic decay results in broad molecular spectroscopic features. This first observation motivated numerous studies of resonant-Auger spectra from core-excited hydrogen-containing molecules, and fast dissociation processes have since been identified in several cases, such as HI,[2] HF,[3] HCl,[4,5] and H_2S.[6,7] In the case of H_2S, experimental resonant-Auger spectra[6] together with theoretical investigations of the topology of the intermediate core-excited states[7] clearly revealed the role of nuclear dynamics during the lifetime of the sulfur $2p^{-1}$ core-excited states. However, the amount of information obtained via electron spectroscopy was limited by the electron analyzers' resolution for the fast Auger electrons. Sharp atomic lines overlap with broad molecular structures making it difficult to distinguish between different transitions in order to describe in detail the competition between neutral dissociation and electronic relaxation. Ion-yield spectroscopy provides an alternate method to investigate the decay channels of core-excited H_2S.[6]

In this article, we report the study of the partial ionic fragmentation pathways following soft-x-ray absorption in the energy region of the S 2*p* ionization thresholds in H_2S. We report the ion-yield spectra of all detectable ionic species, singly and doubly charged cations, as well as anions, for core-level excitation resonances below threshold and for direct core ionization above threshold. Possible fragmentation pathways for all ions are considered in depth.

II. EXPERIMENTAL DETAILS

The measurements were performed using undulator beam line 8.0.1.3 at the Advanced Light Source (Lawrence Berkeley National Laboratory, Berkeley, CA). This undulator beam line is equipped with three interchangeable spherical-gratings, 150, 380, 925 lines/mm, for high resolution and high flux, and provides 6×10^{15} photons/s in the 80–1400 eV photon energy range with a maximum resolving power $(E/\Delta E)<8000$. The grating and slit sizes were chosen to achieve 60 meV resolution at 200 eV photon energy, providing sufficient resolution and photon flux (approximate photon flux of 5×10^{12} photons/s) for a reasonable anion signal. Contamination by third-order light from the undulator passing through the monochromator accounts for less than 1%.

Partial cation and anion yields were obtained with a magnetic mass spectrometer described previously[8] and represented in Fig. 1.

Briefly, the instrument consists of a 180° magnetic mass spectrometer with a resolution of 1 mass in 50,[8] an electrostatic lens to focus the ions created in the interaction region onto the entrance slit of the spectrometer, and an effusive-jet gas cell containing push and extraction plates to move the ions from the interaction region into the lens. Ions are detected with a channel electron multiplier (CEM) at the exit slit of the spectrometer. The polarities of the lens, magnetic field, and CEM may be switched, allowing measurement of either cations or anions produced by photofragmentation. In addition, an analog signal from a capacitance nanometer was recorded simultaneously with the ion signal and incident photon flux to monitor target gas pressure for normalization of the recorded spectra.

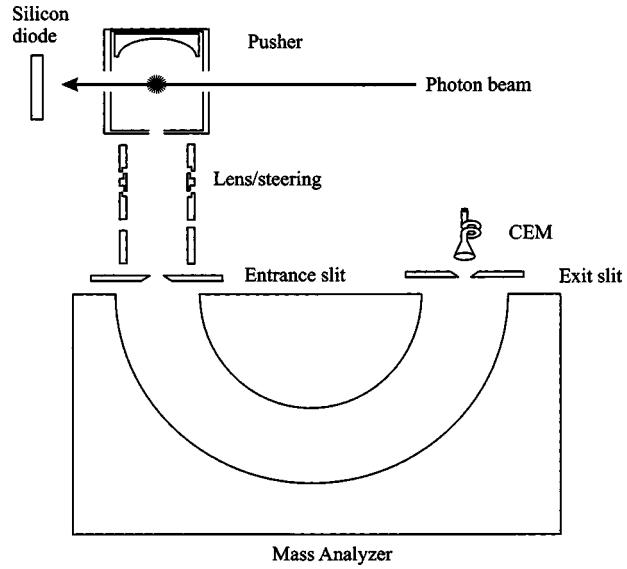

FIG. 1. Schematic representation of the experimental setup used for the partial-ion-yield measurements.

In order to obtain reasonable statistics, most of the spectra presented in this article are the sum of several recordings, which were separately normalized, especially the weaker channels such as the doubly charged ions and the anions, for which up to ten spectra were recorded and summed.

Relative branching-ratio measurements were collected on undulator beam line 7.0.1 at the ALS during two-bunch mode (328 ns period) with a Wiley–McLaren-type time-of-flight (TOF) mass spectrometer. The experimental apparatus used also has been described previously.[9] Voltages on the various lens elements were chosen so there was minimal overlap between the various fragment ions and to ensure all of the energetic fragment ions were collected. The microchannel plate (MCP) detector was kept at -4600 VDC to ensure the ions strike the detector with sufficient energy for maximum detection efficiency, and the discriminator settings set low enough to ensure no mass discrimination was observed. Output pulses from the MCP were fed into a 1 GHz amplifier/constant fraction discriminator (Ortec 9327), with the discriminator setting kept as low as possible. Care was taken when selecting the voltages and discriminator settings to operate the TOF spectrometer under conditions limiting mass/charge transmission dependencies and the transmission was checked using argon. No such dependency was found. However, it is possible that transmission changes still occur, but we assume these changes to be very small and no further correction was made for the transmission. For data acquisition, the discriminator NIM output was fed into a picosecond time analyzer (Ortec 9308). The ion signal was used to start the analyzer and a signal from the storage ring provided a reliable stop pulse. Target gas pressures were in the high 10^{-6} Torr range.

III. RESULTS AND DISCUSSION

In its ground-state geometry, H_2S is bent, with $\theta_{H-S-H}=91.96°$,[7,10] and belongs to the C_{2v} symmetry point group. In the one-electron approximation, the electron configuration for the ground state of H_2S may be written as

$$(1a_1)^2(2a_1)^2(1b_2)^2(3a_1)^2(1b_1)^2(4a_1)^2(2b_2)^2(5a_1)^2(2b_1)^2 \times(6a_1)^0(3b_2)^0{:}X\,{}^1A_1.$$

The $1a_1$ orbital is associated with the S $1s$ core level, and the $2a_1$ with the S $2s$. As in the atomic case, the sulfur $2p$ orbitals split into $2p_{3/2}$ and $2p_{1/2}$ levels due to spin-orbit coupling. The $2p_{3/2}$ is doubly degenerate, but the degeneracy is removed by the anisotropic molecular field of C_{2v} symmetry. The S $2p$ core level thus splits into three components $1b_1$, $3a_1$, and $1b_2$. In the following, we will use notation $L_2-3e_{1/2}$ for the corresponding $2p_{1/2}^{-1}$ threshold, and $L_3-4e_{1/2}$ and $L_3-5e_{1/2}$ for the two $2p_{3/2}^{-1}$ thresholds in accordance with the extended C_{2v} symmetry point group notation used in previous works.[11,12]

Figure 2 shows the partial ion yields recorded for all detectable fragment ions. Four singly charged cations have been measured, H_2S^+, HS^+, S^+, and H^+, and three doubly charged cations, H_2S^{2+}, HS^{2+}, and S^{2+}. Unlike the water molecule for which both O^- and H^- were found,[13] only one negative ion S^- was observed. No signal corresponding to HS^- and H^- could be detected. Calibration of the energy scale was made relative to the high-resolution photoabsorption measurements by Hudson *et al.*,[11] using the well separated $2p_{1/2}\rightarrow 5d$ Rydberg transition measured at 170.94 eV. Normalization of the spectra was made relative to both the photon flux and sample pressure, which were recorded simultaneously with the ion signals. Finally, the background due to direct valence photoionization was subtracted. All the positive fragments are shown on a scale reflecting the branching ratios measured with the TOF apparatus. Because of the large intensity differences observed for the different fragments and for clarity, the singly charged and doubly charged fragments are presented on separate graphs. Although inverting the polarities on the magnet and the steering lens should not affect the detection efficiency, S^- is presented on a separate arbitrary scale.

Detailed assignments of the resonances below threshold have been provided in previous studies using photoabsorption[11,14] and total-ion-yield[10] measurements. The region 163–167 eV, corresponds to one-electron excitations from the sulfur $2p$ core levels to the unoccupied $6a_1$ and $3b_2$ molecular orbitals, resulting from symmetric and antisymmetric combinations of the antibonding S–H orbitals. Due to spin-orbit splitting of the sulfur $2p$ core levels, the resonance feature is composed of four partially overlapping transitions. Using the S^+ partial yield as an example, we show in Fig. 3 the result of a least-squares fit of the resonances in the 163–167 eV region, including four transitions, respectively, centered around the energies: 164.42 eV ($2p_{3/2}\rightarrow 6a_1$), 165.14 eV ($2p_{3/2}\rightarrow 3b_2$), 165.61 eV ($2p_{1/2}\rightarrow 6a_1$), and 166.34 eV ($2p_{1/2}\rightarrow 3b_2$). The spin-orbit splitting deduced from the fit is found to be 1.196 ± 0.024 eV, in excellent agreement with the value 1.201 eV previously reported.[15] The region between 167 eV and the S $2p_{1/2}$ threshold at 171.56 eV has been assigned to both valence-Rydberg mixed states, which is a

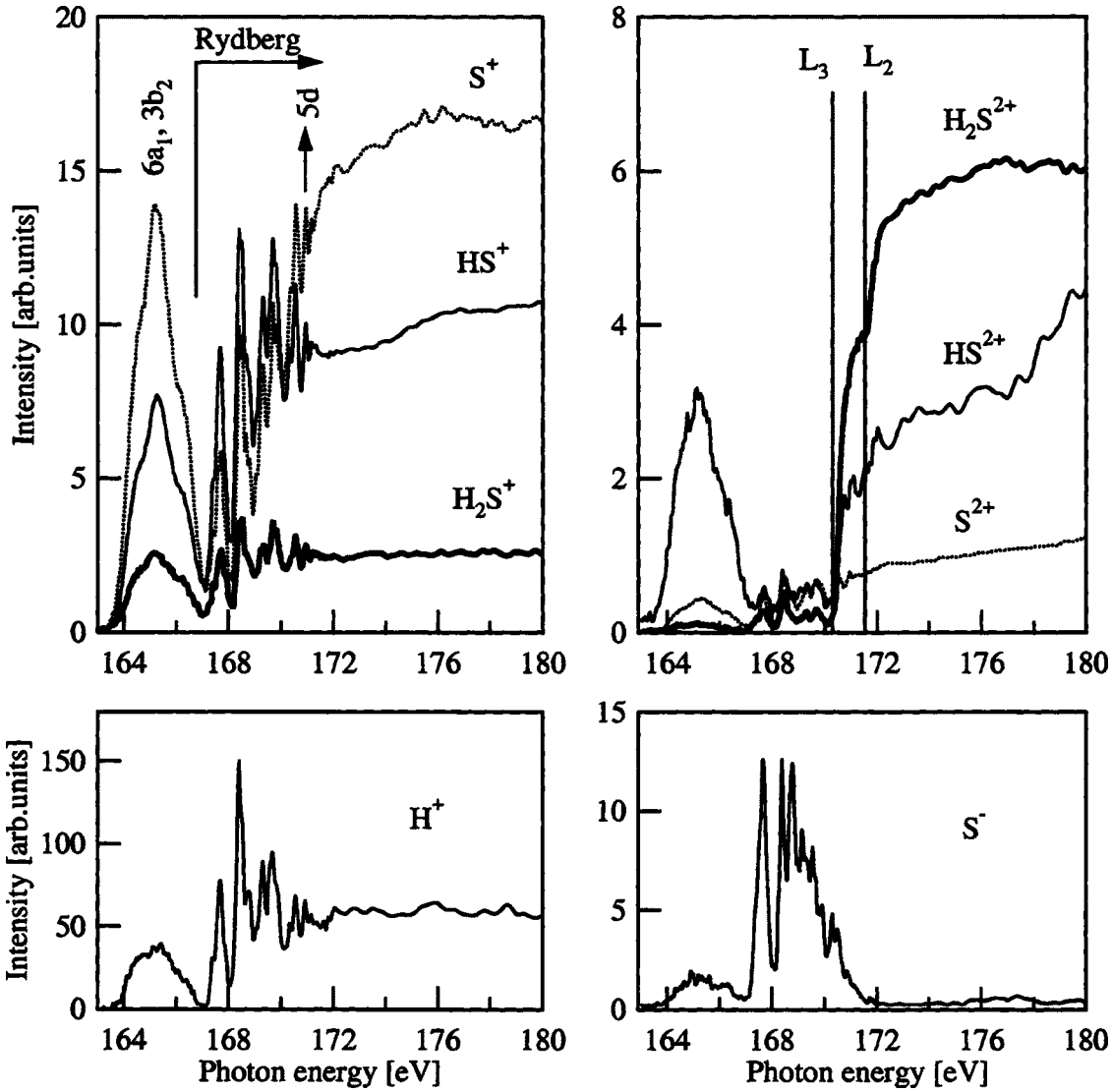

FIG. 2. Partial-ion yields for all detectable fragments in the vicinity of the S $2p$ ionization thresholds. The positive fragments are shown on a scale reflecting the branching ratios measured with the TOF apparatus.

usual feature for hydrogen halides, and pure Rydberg states, and discussed in detail for a high-resolution photoabsorption spectrum.[11]

A. Singly charged cation

Singly charged species below ionization thresholds are primarily produced by resonant-Auger decay. We distinguish two processes: participator decay, leading to final states with one valence hole that can also be reached through direct valence photoionization; and spectator decay, leading to final states with two valence holes and one excited electron. Resonant-Auger spectra of hydrogen halides along core-level resonances involving antibonding molecular orbitals are characterized by atomic lines; the molecule can dissociate before the electronic decay takes place and relaxation of the core would thus occur in a neutral fragment. Instead, if the core electron is excited to a Rydberg orbital, the excited state usually has a bound potential-energy curve in the Franck–Condon region of the ground state[5] and the system decays via molecular resonant-Auger relaxation. For example, to the small overlap of Rydberg orbitals with the core hole, the resonant-Auger spectrum of HCl excited to Rydberg states has been shown to be mainly due to the relaxation of the core-excited HCl parent molecule via spectator decay.[16,17]

To understand the dissociation mechanisms involved in the ion production following $2p$ excitation of H_2S, it is important to compare our results with corresponding resonant-Auger spectra discussed in previous studies.[6,7,12,15,18] Similarly to hydrogen halides, ultrafast dissociation of the $(2p)$ core-excited H_2S^* into HS^* and H fragments, prior to electronic relaxation of the molecule, has been evidenced from the electronic transitions observed in the resonant-Auger spectrum[6,7] after $2p \rightarrow 6a_1, 3b_2$ excitation. Therefore, three contributions to the resonant-Auger spectrum are to be distinguished: participator decay, spectator decay, and decay from the HS^* radical. Participator decay was first considered to be minor,[6] but was later used as the explanation for an observed 75% increase in the intensity of the $4a_1$ line measured upon $2p_{1/2} \rightarrow 3b_2$ excitation.[10]

The ratio between the resonant-Auger decay from the H_2S molecule and from the HS^* radical remains uncertain.

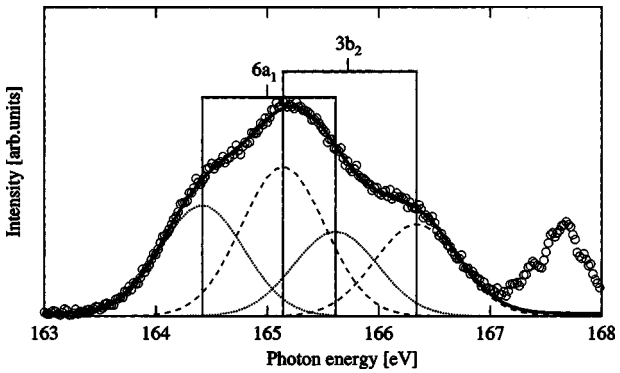

FIG. 3. Least-squares fit of the unresolved $2p_{3/2} \rightarrow 6a_1$, $2p_{3/2} \rightarrow 3b_2$, $2p_{1/2} \rightarrow 6a_1$, and $2p_{1/2} \rightarrow 3b_2$ resonances. Data points are the partial-ion yield of S^+.

Study of the resonant-Auger decay of HCl after Cl $2p$ excitation[19] found up to 55% of the total resonant-Auger intensity is incorporated in the total "molecular background." Although a detailed analysis of the molecular contribution, including participator and spectator decay, versus fragment contribution in the resonant-Auger spectrum of H_2S has yet to be performed, a similar ratio as for HCl is likely. Thus, we expect resonant-Auger decay from the core-excited molecule H_2S^* and the radical HS^* to have roughly equal intensities. From electron-ion coincidence measurements at ionization energies below 40 eV, Brion, Iida, and Thomson[20] obtained the dissociation products and relative branching ratios for the first four ionized states produced by valence ionization of H_2S: $(2b_1)^{-1}$, $(5a_1)^{-1}$, $(2b_2)^{-1}$, and $(4a_1)^{-1}$. Ionization to the $(2b_1)^{-1}$ state was shown to lead exclusively to the production of the parent ion H_2S^+, while the $(5a_1)^{-1}$ state correlates to the production of H_2S^+ (37%) and S^+ (67%). The $(2b_2)^{-1}$ dissociates into HS^+ (95%) and S^+ (5%), and the $(4a_1)^{-1}$ dissociates into S^+ (49%) and H^+ (60%). The same electronic states are populated by participator decay of the core-excited H_2S^* molecule. If we consider that only the $(2b_1)^{-1}$ and $(5a_1)^{-1}$ valence holes lead to the stable parent ion H_2S^+, then the H_2S^+ partial ion yield in Fig. 2 clearly shows that the electronic relaxation of the core-excited molecule is not a weak contribution, in opposition to the statement made in Refs. 6 and 7.

The singly charged ion-yield spectra are clearly dominated by the S^+ fragment. Both HS^+ and S^+ fragments can be created via dissociation of the parent ion following electronic relaxation:

$$H_2S + h\nu \rightarrow H_2S^* \rightarrow H_2S^+ + e^- \tag{1}$$

$$H_2S^+ \rightarrow HS^+ + H$$

$$\rightarrow S^+ + [H + H]. \tag{2}$$

The brackets in pathway (2) indicate molecular H_2 may be formed through excitation of the bending vibrational modes of the molecule in the intermediate excited state, as suggested from potential-surfaces calculations.[7] Both HS^+ and S^+ can be left in excited electronic states and undergo further electronic relaxation to doubly charged ions or, as in the case of HS^+, further dissociation. They can also be created via relaxation of the H_2S^* excited molecule through fast dissociation of the $(2p)^{-1}(6a_1, 3b_2)^{+1}$ core-excited state,

$$H_2S^* \rightarrow HS^* + H$$

$$HS^* \rightarrow HS^+ + e^- \tag{3}$$

for HS^+, and for S^+,

$$H_2S^* \rightarrow S^* + H + H$$

$$S^* \rightarrow S^+ + e^-. \tag{4}$$

The HS^+ partial ion yield includes contributions from both molecular decay, pathway (1), and fragment decay, pathway (3). Based on potential surface calculations of excited states of H_2S and HS, Naves de Brito and Ågren[7] showed pathway (4) is very weak and fast dissociation of the core-excited molecule leads mainly to production of HS^*. Moreover, no electronic transitions corresponding to deexcitation of atomic sulfur has been found in the resonant-Auger spectrum of H_2S,[6] therefore, pathway (4) can be ruled out.

It is interesting to note the production of S^+ is enhanced relative to HS^+ for the $2p \rightarrow 6a_1, 3b_2$ resonances, compared to the Rydberg excitations. In contrast, for water[13] and ethylene and acetylene,[21] the opposite trend was observed: the more-highly dissociated ions are enhanced in the Rydberg region where dissociation is favored by spectator decay after Rydberg excitation. This observation suggests part of the S^+ yield comes from fast dissociation of the molecule at the $6a_1$ and $3b_2$ resonances. An Auger electron/ion coincidence study of the dissociation of H_2S at the $2p \rightarrow 6a_1, 3b_2$ resonance[22] has shown that the HS^+ fragment is created after fast dissociation of H_2S by pathway (3) and relaxation of the HS^+ ion can undergo further dissociation to S^+:

$$H_2S^* \rightarrow HS^* + H$$

$$HS^* \rightarrow HS^+ + e^- \tag{5}$$

$$HS^+ \rightarrow S^+ + H,$$

which enhances the S^+ ion yield along the $2p \rightarrow 6a_1, 3b_2$ resonance.

Above the ionization threshold, the molecule typically emits a photoelectron and an Auger electron, leading to creation of a doubly charged parent ion. Doubly ionized states of small molecules like H_2S usually are dissociative and lead to the production of singly charged ion pairs through the following pathways:

$$H_2S^{+*} \rightarrow H_2S^{2+} + e^- \tag{6}$$

$$H_2S^{2+} \rightarrow HS^+ + H^+$$

$$\rightarrow S^+ + H^+ + H \tag{7}$$

$$\rightarrow S + H^+ + H^+. \tag{8}$$

Except for a small enhancement around 176 eV, discussed below, no particular feature is observed in the singly charged ion yields above threshold or even at the ionization threshold.

B. Doubly charged cation

Below threshold the production of a doubly charged ion is related to the probability of secondary electronic relaxation (Auger cascade) when the singly charged ion created by the primary resonant-Auger decay is left with enough internal energy to undergo further ionization. Although weak, secondary Auger decay of H_2S leads to the pathways

$$H_2S^* \rightarrow H_2S^+ + e^-$$

$$H_2S^+ \rightarrow H_2S^{2+} + e^- \quad (9)$$

$$\rightarrow HS^{2+} + H + e^- \quad (10)$$

$$\rightarrow S^{2+} + H + H + e^-. \quad (11)$$

As generally recognized,[23] the electronic states reached by cascade Auger decay are mostly dissociative. As a consequence HS^{2+} dominates the doubly charged ion yields below threshold; the production efficiency of H_2S^{2+} and S^{2+} below threshold is very small. It is interesting to note we observe a strong enhancement of the HS^{2+} ion yield along the $2p \rightarrow 6a_1, 3b_2$ resonance relative to the Rydberg excitations. The HS^* core-excited radical created after fast dissociation of the neutral molecule can decay to highly excited electronic states of the HS^+ ion, increasing substantially the probability of a secondary Auger decay. The production of HS^{2+} along the $2p \rightarrow 6a_1, 3b_2$ resonance seems to be mainly a product of the dissociation of the molecule prior to electronic relaxation following the three-step pathway:

$$H_2S^* \rightarrow HS^* + H$$

$$HS^* \rightarrow HS^+ + e^- \quad (12)$$

$$HS^+ \rightarrow HS^{2+} + e^-.$$

Part of the S^{2+} yield may come from a similar pathway, as S^{2+} can also be created through a secondary process after relaxation of the HS^* radical. To our knowledge, a conclusive study of doubly charged ions below threshold by means of Auger electron/ion coincidence experiments has never been achieved, although extensive work on this question is needed to clarify the dynamics of these second-order processes.

Unlike the case of singly charged ions, the region immediately above the $L_{2,3}$ ionization thresholds can be analyzed from the H_2S^{2+} parent ion yield shown in Fig. 4. The production of the stable doubly charged parent ion is minor below threshold but dominates the doubly charged partial ion yields above threshold, clearly showing the thresholds. The production of H_2S^{2+} is moderated by postcollision interaction (PCI) in the region immediately above threshold: the slow moving $2p$ photoelectron experiences Coulomb interaction with a doubly charged ion created by the Auger relaxation subsequent to core-level photoelectron emission. The amount of H_2S^{2+} created just above threshold depends on the photoelectron recapture probability. We used the semiclassical PCI model of Armen and Levin[24] to calculate the escape probability of the photoelectron P_{exc} as a function of the excess energy $E_{exc}=h\nu-E(\mathrm{IP})$, where $h\nu$ and $E(\mathrm{IP})$ are the photon energy and ionization energy, respectively. The same approach has previously been used to describe the PCI moderated formation of the negative ion O^- after C $1s$ excitation in CO.[25] Because the semiclassical PCI model has been specifically created to describe atomic PCI, some modifications were made to account for the spin-orbit splitting and molecular-field splitting of the $2p$ core levels, leading to three thresholds: $L_2 3e_{1/2}(2p_{1/2})$, $L_3 4e_{1/2}$, and $L_3 5e_{1/2}$ $(2p_{3/2})$. The molecular-field splitting has been measured to be $\sim$110 meV from high-Rydberg-states analysis[11] and high-resolution photoelectron spectroscopy.[12] This energy splitting should also be seen in the present partial ion yield recorded with a photon bandwidth of 60 meV. Moreover, the H_2S^{+*} parent ion can be left in different vibrational levels after photoionization, and multiple vibrational excitations were taken into account. We used the vibrational components, energy spacing, and related intensities derived from photoelectron measurements (Table I in Ref. 12). The result of the least-squares fit is shown in Fig. 4, and was obtained by combining all the contributions mentioned above in one formula,

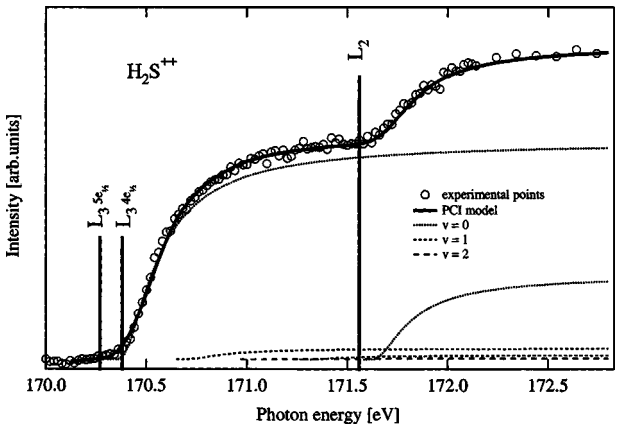

FIG. 4. Partial-ion yield of H_2S^{2+} in the vicinity of the $L_2 3e_{1/2}(2p_{1/2})$, $L_3 4e_{1/2}$, and $L_3 5e_{1/2}(2p_{3/2})$ thresholds (vertical bars). The solid curve is a least-squares fit based on a semiclassical atomic PCI model, modified to take into account the three thresholds and vibrational components (see text for details).

$$I \propto A \exp\{-\Gamma/[\sqrt{2}(x - E_{5e_{1/2}})^{3/2}]\} \quad (13a)$$

$$+ A0.05 \exp\{-\Gamma/[\sqrt{2}(x - E_{5e_{1/2}} - 0.340)^{3/2}]\} \quad (13b)$$

$$+ B \exp\{-\Gamma/[\sqrt{2}(x - E_{4e_{1/2}})^{3/2}]\} \quad (13c)$$

$$+ B0.05 \exp\{-\Gamma/[\sqrt{2}(x - E_{4e_{1/2}} - 0.340)^{3/2}]\} \quad (13d)$$

$$+ C \exp\{-\Gamma/[\sqrt{2}(x - E_{3e_{1/2}})^{3/2}]\} \quad (13e)$$

$$+ C0.05 \exp\{-\Gamma/[\sqrt{2}(x - E_{3e_{1/2}} - 0.340)^{3/2}]\} \quad (13f)$$

$$+ C0.01 \exp\{-\Gamma/[\sqrt{2}(x - E_{3e_{1/2}} - 0.600)^{3/2}]\}, \quad (13g)$$

convoluted with the photon bandwidth (60 meV) to fit the experimental data from the H_2S^{2+} partial ion yield. Equations

(13a) and (13b) correspond to the v=0 and v=1 vibrational levels, respectively, of the $5e_{1/2}$ photoelectrons; Eqs. (13c) and (13d) correspond to the v=0 and v=1 vibrational levels, respectively, of the $4e_{1/2}$ photoelectrons; Eqs. (13e)–(13g) correspond to the v=0, v=1, and v=2 vibrational levels, respectively, of the $3e_{1/2}$ photoelectrons. The amplitudes A, B and C, the core-hold lifetime Γ and the threshold energies, $E_{5e_{1/2}}$, $E_{4e_{1/2}}$, and $E_{3e_{1/2}}$ were parameters in the fit.

The least-squares fit was optimized for $B \rightarrow 0$, indicating, unlike the $5e_{1/2}$ and $3e_{1/2}$ thresholds, the opening of the $4e_{1/2}$ threshold does not influence the formation of the doubly charged parent ion. Such a conclusion might seem surprising, but one can turn to the normal-Auger spectrum to understand suppression of the $4e_{1/2}$ threshold in the H_2S^{2+} parital ion yield. The high-resolution spectrum[12] for Auger S $2p^{-1} \rightarrow X\,^1A_1(2b_1^{-2})$ transitions, corresponding to nonradiative relaxation of core-ionized H_2S^+ ion to the ground state of the doubly charged parent ion H_2S^{2+}, showed an anomalous ratio for the decay from the $4e_{1/2}$ and $5e_{1/2}$ levels: only the decay from the $5e_{1/2}$ level was observed in the spectrum. This issue was later addressed by Gel'mukhanov and Ågren[26] and can be understood in terms of orthogonality of the core $2p_{3/2}(4e_{1/2})$ and valence $2b_1$ molecular orbitals. The amplitude of the Auger decay has a maximum value when both orbitals have the same orientation in space, and minimum when the orbitals are orthogonal. In the case of H_2S the $2b_1$ valence orbital is oriented along the x axis of the molecular frame, with the molecule lying in the zy plane, while the contribution of the sulfur $2p_x$ orbital of the $4e_{1/2}$ sublevel is very small, causing a depression of the $2b_1 \rightarrow 4e_{1/2}$ transition. The suppression of the $4e_{1/2}$ threshold in the H_2S^{2+} partial ion yield indicates the stable doubly charged parent ion is mainly produced through nonradiative decay to the $X\,^1A_1(2b_1^{-2})$ state.

Finally, the fitting procedure employed provides a direct experimental determination of the energy of $5e_{1/2}$ and $3e_{1/2}$ thresholds: 170.30±0.01 eV and 171.56±0.01 eV, respectively, with a spin-orbit splitting of 1.26±0.01 eV, in excellent agreement with the previously reported values 170.303 eV and 171.564 eV (Ref. 11) and 1.259 eV (Ref. 12) and 1.261 eV,[11] respectively. The intensity ratio $(2p_{3/2}/2p_{1/2}) = 2.8$ is larger than the statistical values, and has already been observed (2.5) by Svensson *et al.*[12] in Auger decay.

C. Anions

As for the production of singly charged cations, anions can be produced below threshold through resonant-Auger decay. The anion-cation pair production following dissociation of a singly charged ion created after electronic decay requires the formation of a total double positive charge together with the anion to achieve charge balance. Ion pairs can also be produced after radiative decay and dissociation of a neutral molecule. In most cases[13,25,27–32] dissociation of a molecule into anions and cations following radiative decay has been ruled out on the assumption radiative decay is expected to be very small compared to nonradiative decay for light elements. However, the question of the possible contribution of radiative decay to anion formation has never been clearly addressed. Because only the S^- negative fragment is observed for H_2S, the possible fragmentation pathways are

$$\begin{aligned} H_2S^* &\rightarrow H_2S^{+*} + e^- \\ H_2S^{+*} &\rightarrow S^-H^+ + H^+ \end{aligned} \tag{14}$$

for nonradiative decay, and

$$\begin{aligned} H_2S^* &\rightarrow H_2S^* + h\nu \\ H_2S^* &\rightarrow S^-H^+ + H \end{aligned} \tag{15}$$

for radiative decay. Though we cannot entirely rule out pathway (15), our previous studies as well as newly published anion/cation coincidence results[33] seem to indicate that anions are mainly formed by ion pair creation. Unlike positive ions, the pathways leading to the formation of negative ions are usually unique. As a consequence, anion measurements are a sensitive spectroscopic tool.[27] Above threshold, Auger relaxation following ionization leaves a doubly charged molecule. Anion-cation pair production following the dissociation of a doubly charged ion requires the formation of a total triple positive charge together with the anion to achieve charge balance. Neither H^- nor S^{3+} was observed in our measurements. Because charge balance cannot be achieved for S^- from H_2S, the formation of S^- is forbidden above threshold and should not be observed. However, a low intensity of S^- is observable for a large region around 176 eV. Using CO as an example CO,[27] we attribute this feature to doubly excited states which are known to decay through resonant-Auger relaxation, and can lead to the production of S^- along pathway (14). The same enhancement aroung 176 eV is observed in the partial ion yiels of HS^+, S^+, and H_2S^{2+}. As for many molecules photoexcited in the vacuum ultraviolet energy region[34–36] as well as in the soft x-ray energy region,[27–32] anion spectroscopy allows us to clearly identify doubly excited states lying in the photoionization continuum.

IV. SUMMARY

Complementary to previous resonant-Auger studies, we investigated the mechanisms involved in the dissociation of H_2S following S $2p$ core excitation by means of ion spectroscopy. While Auger spectroscopy can provide detailed information on dynamical processes within the lifetime of the intermediate core-excited states, ion spectra provide information on the final products of the electronic decay and dissociation mechanisms. We reported spectra as a function of photon energy for all detectable fragments and the corresponding dissociation pathways have been discussed. By measuring partial ion yields, a more complete picture of all the mechanisms involved, including fine processes like post-collision interaction just above threshold, can be obtained. However, this type of measurement does not distinguish among the several fragmentation pathways leading to the same fragment. Only techniques like Auger electron/ion coincidence measurements can provide a more detailed description of the processes involved.

ACKNOWLEDGMENTS

The authors thank the staff the ALS for their support, and especially thank professor J.A.R. Samson for use of the partial-ion-yield instrument. The research was funded by the National Science Foundation under Award No. PHY-01-40375. The experiments were performed at the Advanced Light Source, which is supported by the Director, Office of Energy Research, Office of Basic Energy Sciences, Materials Sciences Division of the U.S. Department of Energy under Contract No. DE-AC03-76SF00098.

[1]P. Morin and I. Nenner, Phys. Rev. Lett. **56**, 1913 (1986).
[2]P. Morin and I. Nenner, Phys. Scr., T, **T17**, 171 (1987).
[3]S. Svensson, L. Karlsson, N. Mårtensson, P. Baltzer, and B. Wannberg, J. Electron Spectrosc. Relat. Phenom. **50**, 1 (1990).
[4]H. Aksela, S. Aksela, M. Ala-Korpela, O.-P. Sairanen, M. Hotokka, G. M. Bancroft, K. H. Tan, and J. Tulkki, Phys. Rev. A **41**, 6000 (1990).
[5]H. Aksela, S. Aksela, M. Hotokka, A. Yagishita, and E. Shigemasa, J. Phys. B **25**, 3357 (1992).
[6]H. Aksela, S. Aksela, A. Naves de Brito, G. M. Bancroft, and K. H. Tan, Phys. Rev. A **45**, 7948 (1992).
[7]A. Naves de Brito and H. Ågren H, Phys. Rev. A **45**, 7953 (1992).
[8]W. C. Stolte, Y. Lu, J. A. R. Samson *et al.*, J. Phys. B **30**, 4489 (1997).
[9]J. A. R. Samson, W. C. Stolte, Z.-X. He, J. N. Cutler, Y. Lu, and R. J. Bartlett, Phys. Rev. A **57**, 1906 (1998).
[10]A. Naves de Brito, S. Svensson, S. J. Osborne *et al.*, J. Chem. Phys. **106**, 18 (1997).
[11]E. Hudson, D. A. Shirley, M. Domke, G. Remmers, and G. Kaindl, Phys. Rev. A **49**, 161 (1994).
[12]S. Svensson, A. Ausmees, S. J. Osborne *et al.*, Phys. Rev. Lett. **72**, 3021 (1994).
[13]W. C. Stolte, M. N. Sant'Anna, G. Öhrwall, I. Dominguez-Lopez, L. T. N. Dang, M. N. Piancastelli, and D. W. Lindle, Phys. Rev. A **68**, 022701 (2003).
[14]W. Hayes and F. C. Brown, Phys. Rev. A **6**, 21 (1972).
[15]S. Svensson, A. Naves de Brito, P. Keane, N. Correia, and L. Karlsson, Phys. Rev. A **43**, 6441 (1991).
[16]E. Kukk, H. Aksela, O.-P. Sairanen, E. Nõmmiste, and S. Aksela, Phys. Rev. A **54**, 2121 (1996).
[17]J. Mursu, A. Kivimäki, H. Aksela, and S. Aksela, Phys. Rev. A **58**, R1645 (1998).
[18]A. Cesar, H. Ågren, A. Naves de Brito *et al.*, J. Chem. Phys. **93**, 918 (1990).
[19]E. Kukk, H. Aksela, O.-P. Sairanen *et al.*, J. Chem. Phys. **104**, 4475 (1996).
[20]C. E. Brion, Y. Iida, and J. T. Thomson, Chem. Phys. **101**, 449 (1986).
[21]M. N. Piancastelli, W. C. Stolte, G. Öhrwall, S.-W. Yu, D. Bull, K. Lantz, A. S. Schlachter, and D. W. Lindle, J. Chem. Phys. **117**, 8264 (2002).
[22]K. Le Guen, C. Miron, D. Céolin, R. Guillemin, N. Leclercq, M. Simon, and P. Morin (unpublished).
[23]I. Nenner and P. Morin, *VUV and Soft X-ray Photoionization*, edited by U. Becker and D. A. Shirley (Plenum, New York, 1996), p. 291.
[24]G. B. Armen and J. C. Levin, Phys. Rev. A **56**, 3734 (1997).
[25]D. L. Hansen, W. C. Stolte, O. Hemmers, R. Guillemin, and D. W. Lindle, J. Phys. B **35**, L381 (2002).
[26]F. Gel'mukhanov, H. Ågren, S. Svensson, H. Aksela, and S. Aksela Phys. Rev. A **53**, 1379 (1996).
[27]W. C. Stolte, D. L. Hanson, I. Dominguez Lopez *et al.*, Phys. Rev. Lett. **86**, 4504 (2001).
[28]W. C. Stolte, G. Öhrwall, M. N. Sant'Anna, I. Dominguez Lopez, L. T. N. Dang, M. N. Piancastelli, and D. W. Lindle, J. Phys. B **35**, L253 (2002).
[29]G. Öhrwall, M. N. Sant'Anna, W. C. Stolte, I. Dominguez Lopez, L. T. N. Dang, A. S. Schlachter, and D. W. Lindle, J. Phys. B **35**, 4543 (2002).
[30]S.-W. Yu, W. C. Stolte, G. Öhrwall, R. Guillemin, M. N. Piancastelli, and D. W. Lindle, J. Phys. B **36**, 1255 (2003).
[31]S.-W. Yu, W. C. Stolte, R. Guillemin, G. Öhrwall, I. C. Tran, M. N. Piancastelli, R. Feng, and D. W. Lindle, J. Phys. B **367**, 3583 (2004).
[32]S. W. J. Scully, R. A. Mackie, R. Browning, K. F. Dunn, and C. J. Latimer, J. Phys. B **35**, 2703 (2002).
[33]E. Rühl and R. Flesch, J. Chem. Phys. **121**, 5322 (2004).
[34]K. Mitsuke, S. Suzuki, T. Imamura, and I. Koyano, J. Chem. Phys. **95**, 2398 (1991).
[35]S. Suzuki, K. Mitsuke, T. Imamura, and I. Koyano, J. Chem. Phys. **96**, 7500 (1992).
[36]H. Yoshida and K. Mitsuke, J. Chem. Phys. **100**, 8817 (1994).